Hearing Research 298 (2013) 80–92

Contents lists available at SciVerse ScienceDirect

Hearing Research

journal homepage: www.elsevier.com/locate/heares

Research paper

Response properties underlying selectivity for the rate of frequency modulated sweeps in the auditory cortex of the mouse

Michael Trujillo, Maria Magdalena Carrasco, Khaleel Razak*

Neuroscience Program and Psychology Department, University of California, Riverside, CA 92521, USA

ARTICLE INFO

Article history:
Received 19 August 2012
Received in revised form
10 December 2012
Accepted 21 December 2012
Available online 20 January 2013

ABSTRACT

This study focused on the response properties underlying selectivity for the rate of frequency modulated (FM) sweeps in the auditory cortex of anesthetized C57bl/6 (C57) mice. Linear downward FM sweeps with rates between 0.08 and 20 kHz/ms were tested. We show that at least two different response properties predict FM rate selectivity: sideband inhibition and duration tuning. Sideband inhibition was determined using the two-tone inhibition paradigm in which excitatory and inhibitory tones were presented with different delays. Sideband inhibition was present in the majority (88%, $n = 53$) of neurons. The spectrotemporal properties of sideband inhibition predicted rate selectivity and exclusion of the sideband from the sweep reduced/eliminated rate tuning. The second property predictive of sweep rate selectivity was duration tuning for tones. Theoretically, if a neuron is selective for the duration that a sweep spends in the excitatory frequency tuning curve, then rate selectivity will ensue. Duration tuning for excitatory tones was present and predicted rate selectivity in ~34% of neurons ($n = 97$). Both sideband inhibition and duration tuning predicted rate selectivity equally well, but sideband inhibition was present in a larger percentage of neurons suggesting that it is the dominant mechanism in the C57 mouse auditory cortex. Similar mechanisms shape sweep rate selectivity in the auditory system of bats and mice and movement-velocity selectivity in the visual system, suggesting similar solutions to analogous problems across sensory systems. This study provides baseline data on basic spectrotemporal processing in the C57 strain for elucidation of changes that occur in presbycusis.

1. Introduction

Frequency modulated (FM) sweeps are relatively simple sounds that can serve as probes to understand fundamental mechanisms of spectrotemporal processing in the auditory system. Beginning with the work of Suga (1965) and Whitfield and Evans (1965), it is established that the auditory cortex of all species examined contains neurons selective for the rate and/or direction of FM sweeps (Atencio et al., 2007; Brown and Harrison, 2009; Godey et al., 2005; Hall et al., 2000; Heil et al., 1992; Mendelson and Cynader, 1985; Nelken and Versnel, 2000; Razak and Fuzessery, 2006; Tian and Rauschecker, 2004; Washington and Kanwal, 2008; Zhang et al., 2003). Behavioral studies have shown that rodents discriminate FM sweep direction in a sweep rate-specific manner and that the auditory cortex is necessary for this behavior (Ohl et al., 1999; Wetzel et al., 1998). FM sweep rate and direction selectivity is present in the mouse auditory cortex as well, with the dominant feature being selectivity for a narrow range of FM sweep rates (Trujillo et al., 2011). The present study focused on the mechanisms underlying such selectivity.

The mouse is a useful model system to study sensory processing due to the available genetic engineering techniques to investigate relative contributions of activity-dependent and -independent factors in circuit formation and plasticity (Barkat et al., 2011; Galindo-Leon et al., 2009; Holmstrom et al., 2010; Linden et al., 2003; Linden and Schreiner, 2003; Liu, 2006; Mataga et al., 2001; Morishita et al., 2010; O'Connor et al., 2009; Sugiyama et al., 2008). The strong selectivity for FM sweep rates in the mouse auditory cortex can serve as a physiological probe to study basic circuitry as well as development and disease models of auditory processing. An understanding of the mechanisms underlying FM rate selectivity in the mouse auditory cortex will facilitate inquiries of not just whether selectivity changes during development or because of genetic disorders, but will also provide insights on underlying cellular substrates.

The main motivation for this study was to elucidate FM rate processing mechanisms in the young C57bl/6 strain mouse as a baseline for future studies on how presbycusis influences spectrotemporal processing (Erway et al., 1993; Johnson et al., 1997,

* Corresponding author. Psychology Department, University of California, 900, University Avenue, Riverside, CA 92521, USA. Tel.: +1 951 827 5060.
E-mail address: khaleel@ucr.edu (K. Razak).

0378-5955/$ – see front matter © 2013 Elsevier B.V. All rights reserved.
http://dx.doi.org/10.1016/j.heares.2012.12.013

2000; Noben-Trauth et al., 2003). It is known based on studies of FM sweep responses in several species that the spectrotemporal interactions between the excitatory and inhibitory subcomponents of the frequency receptive field predict rate and direction selectivity (Atencio et al., 2007; Gittelman and Li, 2011; Gittelman and Pollak, 2011; Gordon and O'Neill, 1998; Phillips et al., 1985; Nelken and Versnel, 2000; Razak and Fuzessery, 2006, 2008, 2006; Shamma et al., 1993; Suga, 1965). Given that two important changes in presbycusis are declines in spectrotemporal processing (Frisina and Frisina, 1997) and inhibitory neurotransmission (Caspary et al., 2008; Martin del Campo et al., 2012; Ouda et al., 2008), analysis of mechanisms of FM processing in the C57 strain mice will provide a model system to determine the relationship between the two observed deficits.

The focus of this study was on two different response properties known to predict FM sweep rate selectivity (Gordon and O'Neill, 1998; Fuzessery et al., 2006; Razak and Fuzessery, 2006, 2008). The first property, sideband inhibition, can be determined using the two-tone inhibition paradigm. In this paradigm, excitatory and inhibitory tones are presented with various delays to identify the spectral and temporal properties of sideband inhibition (Brosch and Schreiner, 1997; Calford and Semple, 1995; Fuzessery et al., 2006; Razak and Fuzessery, 2006). In the pallid bat auditory cortex, a delayed high-frequency sideband inhibition (inhibition near the high-frequency edge of the tuning curve) shaped rate selectivity for downward FM sweeps (Razak and Fuzessery, 2006). Downward sweeps with fast sweep rates can reach the excitatory frequencies before the delayed inhibition arrives, eliciting an excitatory response. For slow downward sweeps, the delayed inhibition has sufficient time to arrive to the neuron simultaneously or before the excitation and reduces responses. The timing and bandwidth of high-frequency inhibitory sidebands predicted rate selectivity for downward sweeps. The properties of sideband inhibition in relation to FM rate selectivity are unknown in any other species, and form a key objective of this study.

The second response property predictive of FM rate selectivity is tone duration tuning (Fuzessery et al., 2006). Tone duration tuning is present in auditory systems across vertebrate taxa (Brand et al., 2000; Casseday et al., 1994; Ehrlich et al., 1997; Feng et al., 1990; Gooler and Feng, 1992). Sweeps of different rates spend different durations within the excitatory and inhibitory components of the frequency tuning curve. If a neuron is tuned to the duration of excitatory tones, then sweeps of different rates may elicit different responses. The best sweep rate may be the one that spends the optimal duration within the tuning curve. In the pallid bat inferior colliculus (IC) duration tuning predicted rate selectivity in nearly 50% of the neurons (Fuzessery et al., 2006) suggesting that tone duration tuning plays a role in spectrotemporal processing underlying FM rate selectivity. However, this mechanism was absent in the pallid bat auditory cortex (Razak and Fuzessery, 2006). It remains unclear if the mouse auditory cortex contains tone duration tuning that explains FM rate selectivity.

The primary aim of this study was to determine the relative contributions of sideband inhibition and duration tuning to FM rate selectivity observed in the mouse auditory cortex. Both primary auditory cortex (A1) and anterior auditory field (AAF) were studied. We show that sideband inhibition shapes FM rate selectivity in the majority of neurons in the core fields of the mouse auditory cortex. Duration tuning is important in a minority of neurons. A small number of neurons exhibited both mechanisms.

2. Methods

Mice (C57bl/6 strain, age 30–83 days, $n = 59$ of either sex) were obtained from an in-house breeding colony that originated from Jackson Laboratory (Bar Harbor, Maine). Two to five littermates were housed in each cage under a 12/12 light/dark cycle and fed *ad libitum*. This strain shows accelerated age-related hearing loss (Henry and Chole, 1980; Hunter and Willott, 1987; Mikaelian, 1979; Spongr et al., 1997; Willott, 1986). This can begin as early as 2 months of age, although audiometric evidence of hearing loss appears ~3 months. Taberner and Liberman (2005) compared auditory nerve fiber responses between C57bl/6 (~4 month) and CBA strains (age between 2 and 4 months) and found no differences in spontaneous rates, tuning curves, rate *versus* level functions, dynamic range, response adaptation, phase-locking, and the relation between spontaneous rate and response properties. Trujillo et al. (2011) showed no differences in FM sweep rate selectivity between 1 and 2 mo old mice and 2–3 mo old mice. Therefore, the data from ages between 30 and 83 days were pooled in the present study. The main reason for choosing the C57 strain for this study was to generate data on response properties that explain spectrotemporal processing in young mice. The ages studied here are before the onset of hearing loss. These data will provide the baseline for future studies with genetic models of human disease on this background strain, such as presbycusis. All procedures were approved by The Institutional Animal Care and Use Committee at the University of California, Riverside.

2.1. Surgical procedures

A combination of ketamine (150 mg/kg) and xylazine (10 mg/kg) was injected (i.p.) to induce anesthesia for surgery. Anesthesia was maintained throughout the experiment by either supplemental doses of ketamine-xylazine or isoflurane inhalation (0.2–0.5% in air). Anesthetic state was assessed via the toe-pinch reflex test throughout the experiment and supplemental anesthetic was administered as needed. After an areflexic state of anesthesia was reached, a midline scalp incision was made and the right temporalis muscle was reflected. A dental drill was used to perform a craniotomy to expose the auditory cortex. At the end of electrophysiological recording, mice were euthanized with pentobarbital sodium (125 mg/kg).

2.2. Acoustic stimulation

All acoustic stimuli, including FM sweeps and tones, were driven and data were acquired by custom software (Batlab, Dr. Don Gans, Kent State University, Kent, OH). The rise and fall times of all sounds used were 1 msec each. In the instances when sounds of 1 msec duration were used, the rise and fall times were 0.5 msec each. Sound intensities between 10 and 80 dB SPL were used and were controlled with programmable attenuators (PA5; Tucker-Davis Technologies, Gainesville, FL) prior to amplification by a stereo amplifier (Parasound HCA1100) or an integrated amplifier (Yamaha AX430). A 1 Hz repetition rate was used for all experiments. Sounds were delivered through a free-field ribbon tweeter (LCY-K100, Madisound, Wisconsin) located 6 inches and 45° from the left ear. All recordings were obtained from the contralateral, right hemisphere. Frequency response of the acoustic stimuli system was flat within ±3 dB for frequencies between 7 and 40 kHz as measured by a ¼ inch Bruel and Kjaer microphone and measuring amplifier. A Krohn-Hite filter (Brockton, MA) was used to filter out frequencies below 5 kHz (Butterworth, 24 dB/octave).

2.3. Electrophysiology

A stereotaxic apparatus (Kopf model 930, California) and bite bar (Kopf model 923B) were used to secure mice for electrophysiological recordings. Experiments were conducted in a sound-attenuated chamber lined with anechoic foam (Gretch-Ken Industries, Oregon). Neurophysiological recordings were acquired

using glass microelectrodes filled with 1M NaCl (2–10 MΩ impedance). Electrodes were driven into the cortex with a Kopf direct drive 2660 micropositioner. Single-unit recordings were obtained between depths of 200 and 560 μm (mean = 358 ± 87.9 μm). Single-unit responses were identified by constancy of amplitude and waveform as displayed on an oscilloscope and were isolated using a time/amplitude window discriminator. Data quantification consisted of counting the number of spikes elicited over 20 stimulus repetitions (1 Hz repetition rate). Poststimulus time histograms (PSTHs) were obtained over a 300 msec window relative to stimulus onset. There is typically little or no spontaneous activity in the anesthetized mouse auditory cortex.

2.4. Data acquisition

The A1 of the C57bl6/j mouse can be identified by vascular landmarks (Willott et al., 1993) as well increasing characteristic frequency (CF) in the caudal to rostral direction (Stiebler et al., 1997; Trujillo et al., 2011). The AAF is located immediately rostral to A1 and exhibits a reversed tonotopy relative to A1. Both A1 and AAF are considered core auditory cortex (Cruikshank et al., 2001). The purpose of the present study was to determine the mechanisms that govern FM sweep rate selectivity in the core auditory cortex; so both A1 and AAF neurons were studied. These neurons can be distinguished from 'non-core' neurons, including those from the ultrasonic field and secondary auditory cortex (AII), based on robust tone responses, narrow tuning and short response latencies. The goal was not to determine if A1 and AAF differed in FM rate mechanisms. Therefore, no effort was made to identify the location of neurons within these two fields. Pure tones (5–50 kHz and 2–30 msec duration), broadband noise and up/down sweeps were used as search stimuli to isolate single neurons. Upon isolation, tone response properties were acquired. Pure tones with frequencies between 5 and 50 kHz (1–5 kHz resolution, 5–10 msec duration) were presented to determine excitatory frequency tuning curves. The CF was noted as the frequency at which the neuron responded to at least five consecutive presentations at the lowest sound intensity tested. The excitatory frequency tuning at 10, 20 and 30 dB above the minimum threshold was then determined by increasing intensity in 10 dB steps and changing frequencies with 1 kHz resolution.

2.5. Frequency modulated sweep rate selectivity

The vast majority of neurons in A1 and AAF of the mouse exhibit CFs <50 kHz (Willott et al., 1993; Trujillo et al., 2011). As the goal of this study was to identify mechanisms of spectrotemporal processing in A1 and AAF, the FM sweeps used were in the 5–50 kHz range. Most neurons in the C57 mouse auditory cortex respond similarly to upward and downward sweeps (Trujillo et al., 2011). Therefore, this study focused on identifying mechanisms of rate selectivity only for downward FM sweeps. Sweep rate selectivity was determined by presenting linear downward FM sweeps of fixed bandwidth and different durations. The sweep rate, defined as the rate of change in kHz/msec, was determined by dividing the sweep bandwidth (in kHz) by the duration (in msec). FM sweeps were presented at a single intensity, 10–20 dB above threshold for excitation with the CF tone. A single intensity above threshold was not used across all neurons because in some cases a strong non-monotonic relationship is present between intensity and response magnitude. The intensity producing the most robust responses was chosen within the range specified above. The sweep bandwidth was chosen to be approximately centered at the excitatory range of frequencies at the amplitude tested. In addition, and unless noted otherwise, the FM sweep bandwidth extended at least 10 kHz outside the high-frequency edge of the tuning curve. This ensures that putative high-frequency inhibitory sidebands, which abut the excitatory tuning curve in A1 (Razak and Fuzessery, 2006; Wu et al., 2008), were included in the downward FM sweep. Sweep durations between 2 and 200 msec were used. This allowed a broad range of FM rates between 0.08 and 20 kHz/ms to be tested. We have shown previously that core cortical neurons in the mouse respond selectively to FM sweep rate and not to sweep duration or sweep bandwidth (Trujillo et al., 2011). Also, neurons respond selectively to sweep rates even at the very short durations used.

Neurons were classified (Fig. 1) as all-pass (AP), band-pass (BP), fast-pass (FP), or slow-pass (SP) according to FM rate selectivity (Felsheim and Ostwald, 1996; Mendelson et al., 1993; Poon et al., 1991; Razak and Fuzessery, 2006; Ricketts et al., 1998; Tian and Rauschecker, 1994; Trujillo et al., 2011). AP neurons respond at above 50% of maximum response for all rates tested (Fig. 1A). These are non-selective neurons and were not studied further. SP neurons were selective for slow FM sweep rates and responses decreased below 50% of maximal response as FM sweep rate was increased (Fig. 1D). Relatively few SP neurons were found in this study, thus mechanisms were not explored in SP neurons. BP neurons were selective for a range of rates, with responses dropping below 50% of maximal response as FM sweep rate was decreased or increased beyond that range (e.g., Fig. 1B). FP neurons were selective for fast FM sweep rates and responses decreased below 50% of maximal response as FM sweep rate was decreased (e.g., Fig. 1C). This study focused on demonstrating the extent to which high-frequency inhibition (HFI) and duration tuning can participate in (or contribute to) mechanisms underlying FP and BP rate selectivity.

Neuronal selectivity for sweep rate was further quantified using the 50% cutoff rate, best rate and rate tuning index (RTI). The 50% cutoff rate was defined as the rate at which response fell to 50% of maximum response. FP neurons have one value of 50% cutoff rate. BP neurons have two such values, one at fast rates ('50% cutoff – fast') and one at slow rates ('50% cutoff – slow'). Best rate (BR) was quantified for BP neurons as the geometric center of the range of FM rates that produced >80% of maximum response. The RTI was calculated as follows (Atencio et al., 2007; Brown and Harrison, 2009; Trujillo et al., 2011):

$$\mathrm{RTI} = (n/n-1) \times [1 - (\mathrm{mean}/\mathrm{max})]$$

where n = the number of FM sweep rates assessed, 'mean' is the average response across all rates tested and 'max' is the maximum response. RTI varies between 0 and 1, with a higher values indicating greater selectivity.

Following identification of neurons with BP or FP rate selectivity, the contributions of sideband inhibition and duration tuning as underlying response properties were assessed as follows:

2.6. Sideband inhibition

The bandwidth and arrival time of high-frequency inhibitory (HFI) sidebands were quantified using a 'two-tone inhibition over time' paradigm (Brosch and Schreiner, 1997; Calford and Semple, 1995; Gordon and O'Neill, 1998; Razak and Fuzessery, 2006). The focus was only on HFI because downward sweeps traverse this sideband before entering the excitatory tuning curve. In the two-tone inhibition paradigm, an excitatory (at the CF) tone and a second tone were presented with different delays between them. The intensities of both tones were the same as the intensity used to determine FM sweep rate selectivity (10–20 dB above response threshold at CF). The CF tone was 5 msec in duration and the second tone was 10 msec in duration. To identify inhibitory frequencies, the two tones were presented with delays of −2 to +10 msec between them. Zero delay indicates simultaneous onset, positive delays indicate delayed CF

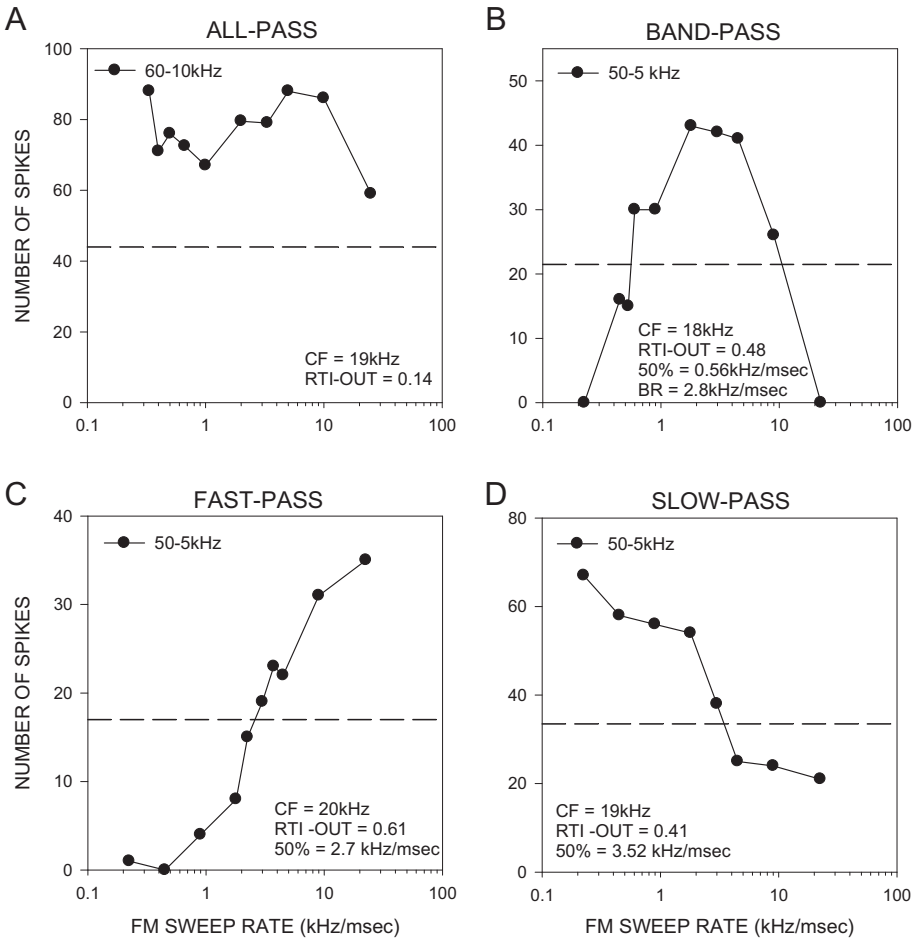

Fig. 1. Classification of FM sweep rate tuning. (A) All-pass (B) Band-pass (C) Fast-pass (D) Slow-pass. The dashed line in each panel marks 50% of maximum response. The 'number of spikes' on the y-axis in this and all subsequent graphs are in response to 20 repetitions of each stimulus. The bandwidth of sweep used is indicated in each panel. CF: characteristic frequency, RTI-out: rate tuning index calculated for sweeps with bandwidths that extended well outside the excitatory tuning curve, BR: best rate for the band-pass neuron, 50%: the 50% cutoff rate for fast-pass and band-pass neurons.

tone relative to the second tone and negative delays indicate that the CF tone was presented first (e.g., Fig. 2A and B).

A qualitative-quantitative sequence was used to identify the HFI sideband. The frequency of the second tone was roved between the highest excitatory frequency of the neuron and 50 kHz with 1–5 kHz resolution. Preliminary data indicated that inhibitory sidebands in most neurons lie just outside the excitatory tuning curve (consistent with Wu et al., 2008). Therefore, frequency of the second tone was varied with 1 kHz resolution near the high-frequency edge of the tuning curve, and with 5 kHz resolution further away. The frequency–delay combinations of the two tones that resulted in a clear decrease (response to less than 2 out of 5 consecutive stimulus repetitions) in response compared to CF tone alone were qualitatively noted as inhibitory. The arrival time of HFI was then quantified by holding the frequency of the second tone at the center of this range of inhibitory frequencies and varying the delay between the two tones (e.g., Fig. 2A and B). Both tones were presented at the same amplitude. The 'arrival time of inhibition' was defined as the shortest delay between the two tones at which the response declined below 50% of response to CF tone alone. The 'bandwidth of inhibitory sideband' was quantified by holding the delay constant and varying the inhibitory tone frequency in 0.5 kHz steps (e.g., Fig. 2G). The constant delay was chosen as the delay of maximum inhibition from the arrival time plot. The range of frequencies of the second tone that reduced responses by at least 50% of CF response was noted as the bandwidth of HFI.

2.7. Duration tuning

The response of neurons to the CF tone with durations between 1 and 200 msec was recorded to determine duration tuning. For the 1 msec tone duration, the rise and fall times were 0.5 msec each. For all other tone durations, the rise/fall times were 1 msec each. Neurons were classified (e.g., Fig. 3) according to duration tuning for CF tones as all-pass-DT, band-pass-DT, short-pass-DT, or long-pass-DT (Fuzessery and Hall, 1999; Fuzessery et al., 2006; Razak and Fuzessery, 2006). 'DT' is used in this paper to distinguish similar classification scheme for FM rate selectivity functions. All-pass-DT neurons responded within 50% of maximum response for all durations. Responses of band-pass-DT neurons declined to at least 50% of maximum response for durations shorter or longer than a preferred duration. The response of short-pass-DT neurons decreased below 50% of maximal response as durations increased. The response of long-pass-DT neurons fell below 50% of maximal response as tone durations decreased.

2.8. Critical tests for sideband inhibition and duration tuning in shaping FM rate selectivity

If HFI shapes downward FM sweep rate selectivity, then removing the HFI from the sweep should reduce or eliminate rate selectivity. A downward FM sweep will exclude the HFI sideband if the sweep starts inside the high-frequency edge of the tuning

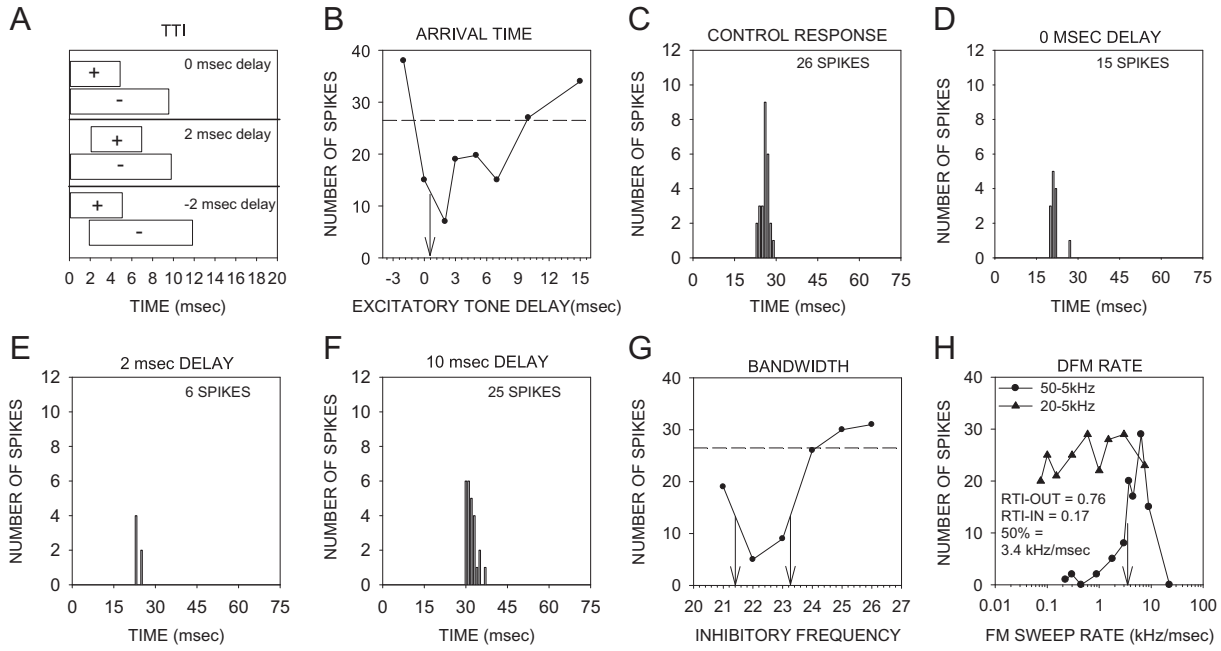

Fig. 2. An example of delayed HFI shaping downward FM rate selectivity. (A) Schematic for the temporal relationships between excitatory and inhibitory tones used in the two-tone inhibition paradigm. The duration of the excitatory and inhibitory tones were 5 and 10 msec, respectively. Positive delays between the two tones indicate that the excitatory (+) tone was delayed relative to the inhibitory (−) tone. Negative delays show the excitatory tone was advanced. Zero delay indicates simultaneous onset of both tones. (B) The two-tone inhibition plot for a HFI tone (23 kHz, 10 msec duration) and an excitatory CF tone (16 kHz, 5 msec duration). The dashed line marks the response to the CF tone presented alone. The vertical arrow shows the delay between the two tones at which response decreases to 50% of CF tone response. This delay, termed 'arrival time of inhibition', was ~0.44 msec in this neuron. The PSTHs at selected delays (C–F) show the time course of two-tone inhibition. Sound onset is at 0 msec. (G) The bandwidth of HFI was determined by changing the frequency of the inhibitory tone while the delay between the two tones was fixed at the best delay (2 msec) identified in (B). The frequency range that suppressed response of the neuron by at least 50% of CF-alone response was considered bandwidth of HFI. The HFI bandwidth of this neuron (indicated by the vertical arrows) was 2 kHz. (H) The neuron was strongly rate selective (RTI-out = 0.76) when the sweep bandwidth included the HFI (the 50–5 kHz sweep). The neuron lost rate selectivity (RTI-in = 0.17) when the sweep excluded HFI (the 20–5 kHz sweep).

curve. The rate tuning index (RTI) can be used to compare rate selectivity for FM sweeps that include and exclude the HFI. The degree to which RTI for downward sweeps declines with the exclusion of HFI indicates the contribution of HFI in shaping rate selectivity for such sweeps.

Duration tuning for tones can explain FM rate selectivity (Fuzessery et al., 2006). Duration tuning for tones is based on the interactions between excitation and inhibition generated by the tone (Casseday et al., 2000, 1994; Fuzessery and Hall, 1999). Therefore, if this mechanism was acting alone, the exclusion of putative sideband inhibition should not influence rate tuning. The RTI values for downward FM sweeps that include or exclude sideband inhibition should be similar if duration tuning was the mechanism. Based on these conceptual grounds, the RTI was compared for sweeps that included and excluded HFI to determine whether sideband inhibition or duration tuning was involved in shaping rate selectivity. The abbreviation 'RTI-out' denotes that RTI was calculated for sweeps that started outside the tuning curve and, therefore, included putative HFI. The abbreviation 'RTI-in' indicates that the sweep excluded putative HFI sidebands by starting inside the tuning curve.

3. Results

The main aim of this study was to identify the contributions of sideband inhibition and tone duration tuning to fast-pass and band-pass FM rate selectivity in the core auditory cortex (A1/AAF) of the mouse. The focus was only on downward sweeps as most neurons in the mouse auditory cortex respond similarly to up/down sweeps (Trujillo et al., 2011). The focus was also on sweeps with frequencies between 5 and 50 kHz, as the vast majority of neurons in A1/AAF exhibit CF < 50 kHz (Willott et al., 1993; Trujillo et al., 2011). In addition, neurons with CF < 50 kHz show FM sweep rate selectivity (Trujillo et al., 2011). The role of high-frequency sideband inhibition and duration tuning in shaping FM rate selectivity was tested in 53 and 97 neurons, respectively.

3.1. Sideband inhibition

The high frequency inhibitory (HFI) sideband explained downward FM rate selectivity in 47/53 (88.8%) neurons tested. Fig. 2 shows an example. Fig. 2A is a schematic of the two-tone inhibition paradigm. Fig. 2B shows that this neuron exhibited a maximal decline in the two-tone response when the CF tone (16 kHz) was delayed by 2 msec relative to the inhibitory tone (23 kHz). The arrival time, defined as the shortest delay at which response declined to 50% of response to CF tone alone, was ~0.44 msec (Fig. 2B). Fig. 2C–F show PSTHs for the arrival time function depicted in Fig. 2B. The bandwidth of inhibition was obtained by keeping the delay between the two tones constant (at the delay of maximum inhibition, 2 msec for this neuron) and varying the frequency of the inhibitory tone. The range of frequencies that inhibit the response to at least 50% of CF response was noted. Frequencies between 21.5 and 23.5 kHz satisfied the 50% inhibition criterion in this neuron (Fig. 2G). The interaction between HFI bandwidth and arrival time can predict rate selectivity (Razak and Fuzessery, 2006). The 50% cutoff rate is predicted by the following formula:

$$\text{Predicted 50\% cutoff rate} = [\text{HIF} - \text{HEF}]/\text{arrival time}(\text{kHz}/\text{msec})$$

where, HIF is the highest inhibitory frequency (the high-frequency edge of the HFI sideband) and HEF is the highest excitatory

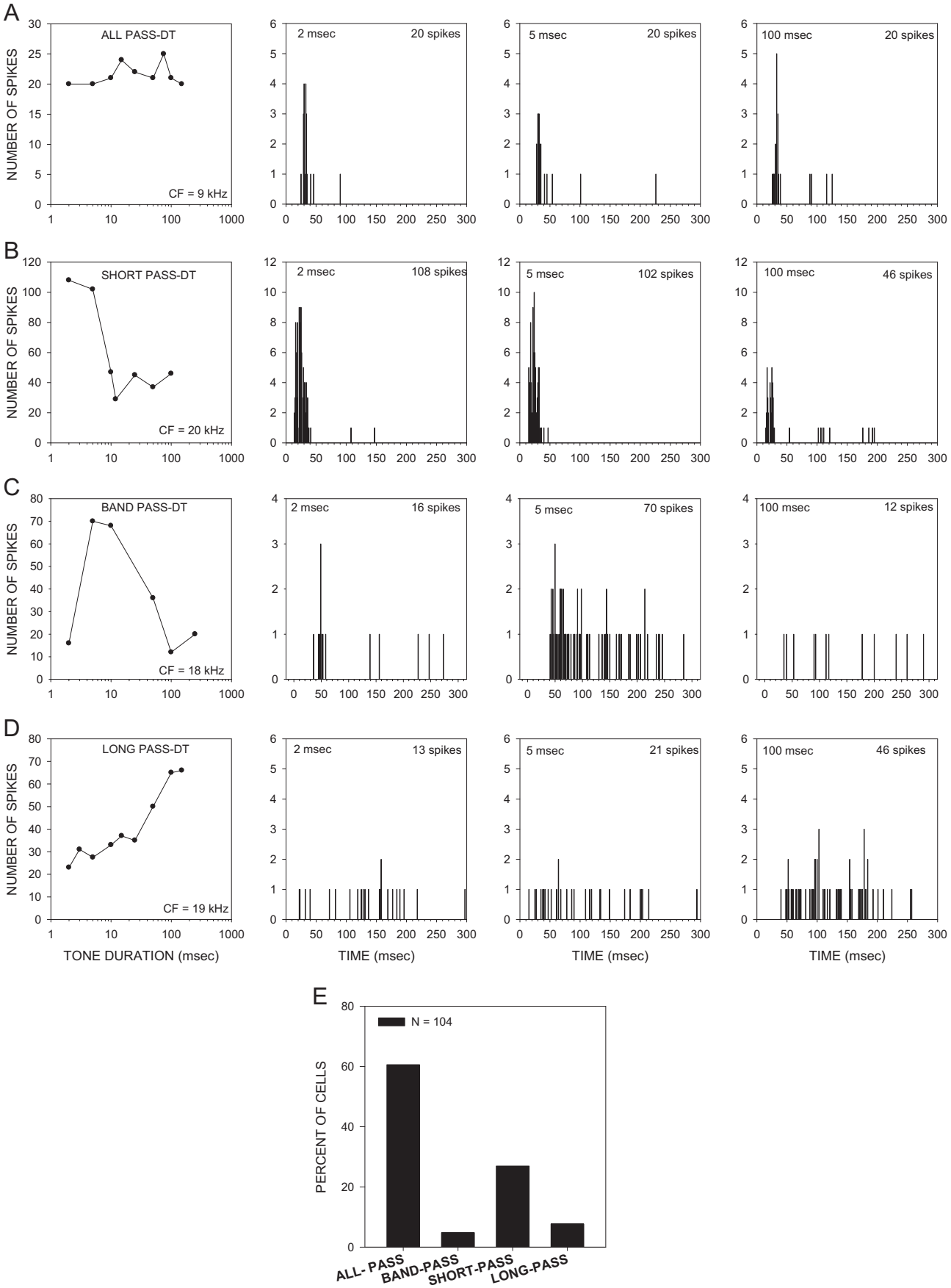

Fig. 3. Classification of duration tuning type in response to CF tone (A) All-pass-DT (B) Short-pass-DT (C) Band-pass-DT (D) Long-Pass-DT. Selected PSTHs are also shown. Tone onset is at 0 msec. (E) The distribution of duration tuning types.

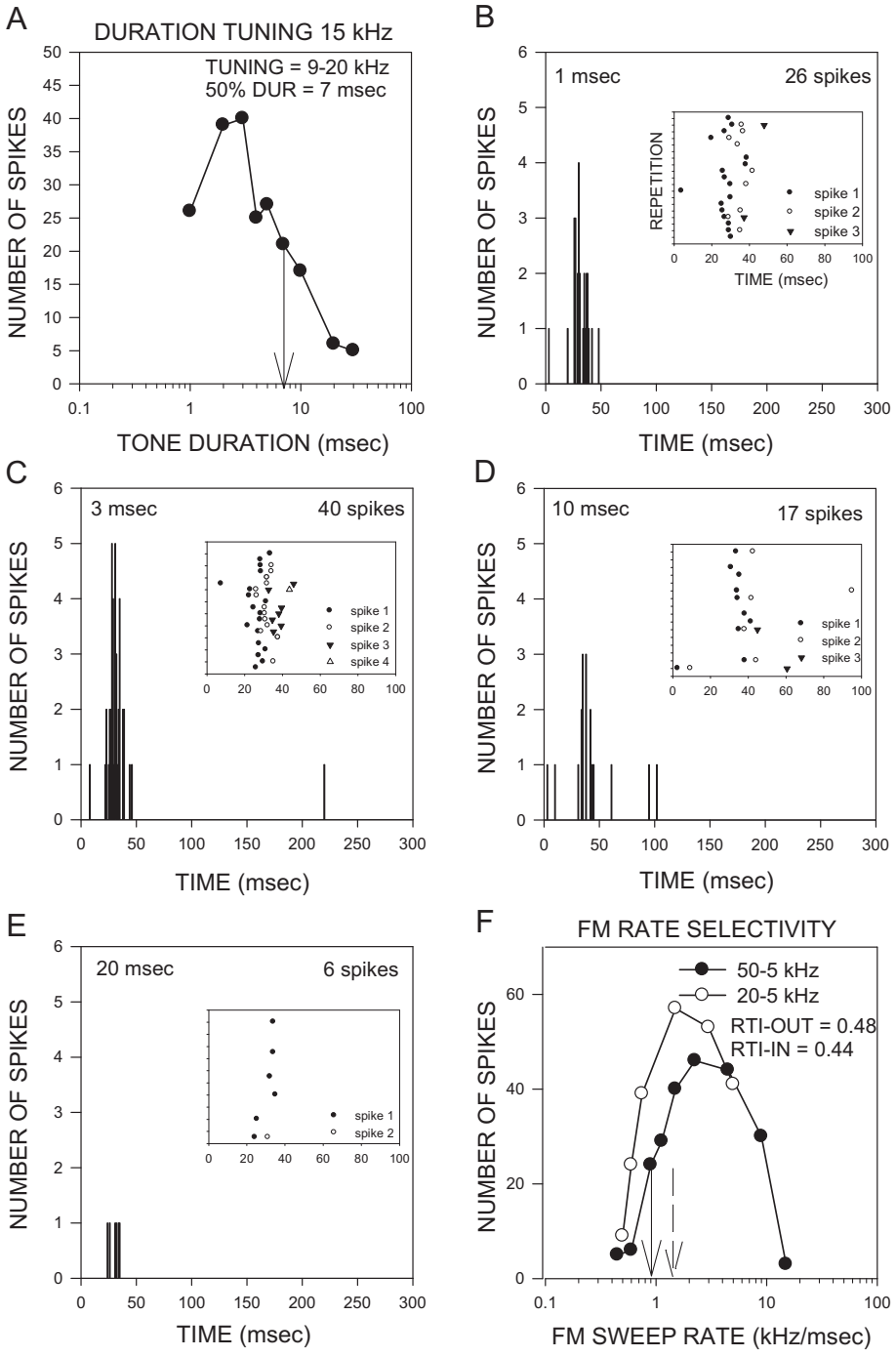

Fig. 4. A neuron in which duration tuning predicts FM rate selectivity. (A) This neuron was tuned to the CF tone (15 kHz) duration with strong responses between 2 and 3 msec. The vertical arrow shows the duration at which the response decline to 50% of maximum. Duration tuning was tested at 15 dB above CF threshold in this neuron. The excitatory tuning of this neuron at this intensity was 9–20 kHz (B–E) Selected PSTHs for the duration tuning function depicted in (A). The insets in these panels show raster plots of spike timing. Each row corresponds to a stimulus repetition. Only the responses within a 100 msec window from stimulus onset are shown. The neuron produced between 0 and 4 spikes for each stimulus repetition. The different symbols in the raster indicate the spike number with the solid circle pointing to the first spike. The relatively small variability in the first spike latency can be seen from these raster plots. (F) When tested with downward FM sweeps, that started well outside the excitatory tuning curve (the 50–5 kHz sweep), the neuron was BP rate selectivity, with preference for rates ~3 kHz/ms. The RTI for the sweep starting outside the tuning curve (RTI-out) was 0.48. When the sweep started inside the tuning curve (the 20–5 kHz sweep), and thus excluded putative sidebands, the neuron was still BP tuned with a best rate ~2 kHz/ms. The RTI for the sweep starting inside the tuning curve (RTI-in) was 0.44, similar to the RTI-out. This indicates that the contribution of putative HFI to rate selectivity was relatively minor in this neuron. The solid arrow depicts the observed 50% cutoff rate of 0.8 kHz/ms and the dashed arrow depicts the predicted 50% cutoff rate of 1.71 kHz/ms.

frequency (high-frequency edge of the excitatory tuning curve) at the intensity at which FM rate selectivity was recorded. The excitatory tuning of the neuron in Fig. 2 at the intensity at which two-tone inhibition was measured was 9–22 kHz. Therefore, the spectral difference between HIF (23.5 kHz) and HEF (22 kHz) was 1.5 kHz. Given the arrival time of 0.44 kHz/ms, the predicted 50% cutoff was 3.41 kHz/ms (1.5 kHz/0.44 msec). Fig. 2H shows the observed FM rate selectivity function for this neuron. When the

sweep included the HFI (the 50–5 kHz sweep) the actual 50% cutoff rate was 3.41 kHz/ms, the same as the predicted value. When the sweep excluded the HFI by starting inside the excitatory tuning curve (the 20–5 kHz sweep), the neuron lost rate selectivity (Fig. 2H) indicating that the HFI was necessary for rate selectivity in this neuron.

HFI was quantified using the two-tone inhibition paradigm in 53 neurons that were BP or FP rate selective. HFI was found in the majority of these neurons (88%, 47/53). The mean arrival time and bandwidth of HFI were 2.62 ± 2.2 msec and 4.26 ± 2.4 kHz, respectively ($n = 47$). There was no correlation between CF and arrival time ($r^2 = 0.09$, $p > 0.05$) or bandwidth ($r^2 = 0.07$, $p > 0.05$) of HFI sideband, suggesting that similar HFI properties are found across the tonotopic axis. This also accounts for a lack of CF-dependency in FM rate selectivity in the C57 mouse (Trujillo et al., 2011). In these 47 neurons, the actual FM rate selectivity functions were also recorded, facilitating a comparison of predicted and observed rate selectivity. There was a strong correlation between the predicted and observed 50% cutoff rate (Fig. 5A, Pearson correlation, $r = 0.73$, $p < 0.001$).

In 36/47 neurons with identified HFI, the critical test for the contribution of sideband inhibition to rate selectivity was performed. That is, rate selectivity index for sweeps that included the HFI (RTI-out) was compared with rate selectivity index when HFI was excluded (RTI-in). The mean RTI-in was significantly lower than the mean RTI-out (Fig. 6A, paired t-test, $t = 9.22$, $p < 0.001$, $\eta^2 = 0.84$) indicating that exclusion of HFI from the sweep significantly reduced rate tuning in these neurons. For the age range studied (30–83 day old mice), there was no correlation between age of mouse and HFI arrival time ($r^2 = 0.08$, $p > 0.05$) or HFI bandwidth ($r^2 = 0.03$, $p > 0.05$). Therefore, the observed data were not influenced by possible hearing loss in this strain within the age range studied. The lack of difference in sideband properties with age in the young mice may also account for similarities in FM rate selectivity observed between 30–60 and 61–90 day old mice (Trujillo et al., 2011). Together, these data indicate that HFI was present in the majority of BP/FP neurons, the properties of HFI predicted rate selectivity and exclusion of HFI reduces rate selectivity.

3.2. Duration tuning

Duration tuning for CF tones was examined in 97 BP/FP neurons. Fig. 3 provides examples and associated PSTHs for the four different types of duration tuning observed in this study. All neurons recorded in this study responded to the onset of tones in a manner similar to the examples shown (Fig. 3). No offset responders were found. Fig. 3E shows the distribution of the different duration tuning types. The majority (60%) of neurons were all-pass-DT (non-selective for tone duration). A third of the population (33/97) exhibited short-pass-DT or band-pass-DT in the core auditory cortex of the mouse. Note that this distribution is only for neurons with FP/BP sweep rate selectivity and may not reflect duration tuning characteristics of the core auditory cortex of the mouse.

Fig. 4 depicts a neuron in which short-pass duration tuning predicted FM sweep rate selectivity. The neuron was selective for the duration of the CF tone, with a best duration of ~2.2 msec (Fig. 4A). The 50% cutoff duration was 7 msec indicating tone durations longer than 7 msec elicited <50% of maximum response. Selected PSTHs (Fig. 4B–E) show responses to different tone durations. The excitatory tuning bandwidth of this neuron at the intensity at which duration tuning was determined was 20–9 kHz (inclusive excitatory bandwidth = 12 kHz). Using the method of Fuzessery et al. (2006), the 50% cutoff sweep rate and best sweep rate for downward FM can be predicted as follows:

$$\text{Predicted 50\% cutoff} = [\text{Excitatory Bandwidth} / \text{50\% cutoff duration for pure tones}]$$

$$\text{Predicted Best Rate} = [\text{Excitatory Bandwidth} / \text{best duration for pure tones}]$$

For the neuron in Fig. 4, the predicted 50% cutoff was 1.71 kHz/ms (12 kHz/7 msec, dashed arrow in 4F). The predicted best rate was 5.4 kHz/ms (12 kHz/2.2 msec). The observed 50% cutoff and best rate for the neuron depicted were 0.8 kHz/ms and 3.08 kHz/ms respectively (Fig. 4F). Whether HFI was also present in this neuron was not tested. However, exclusion of putative HFI by starting the sweep inside the tuning curve (the 20–5 kHz/ms sweep), did not reduce rate tuning (the RTI-in and RTI-out were similar, Fig. 4F). This indicates that mechanisms within the excitatory tuning curve, and not HFI, shaped FM sweep rate tuning in this neuron. The prediction data suggest that duration tuning is the likely underlying mechanism.

Of the 97 BP/FP sweep selective neurons, 33 (34%) were either short-pass-DT or band-pass-DT. In these 33 neurons, the excitatory frequency tuning curves and actual FM rate selectivity functions were also recorded, facilitating a comparison of predicted and observed FM rate selectivity. Fig. 5B demonstrates that predicted 50% cutoff rate based on duration tuning is correlated with observed 50% cutoff rate ($r = 0.53$, $p < 0.01$), Fig. 5C demonstrates that the predicted and observed best rate of band-pass neurons were also correlated ($r = 0.39$, $p < 0.05$). These data indicate that tone duration tuning can predict rate selectivity in the mouse auditory cortex.

We predicted that across the population, the RTI-out and RTI-in of neurons in which duration tuning predicted rate selectivity will be similar (as in the example shown in Fig. 4). That is, in duration-tuned neurons, HFI will play a minimal role in FM rate selectivity. However, in the 21 short-pass-DT neurons in which RTI-in and RTI-out were also determined, there was a reduction in RTI-in compared to RTI-out (Fig. 6A, $t = 2.92$, $p < 0.01$, $\eta^2 = 0.56$). This suggests that putative HFI may contribute to rate selectivity in these neurons as well. A comparison of effect sizes reveals that the reduction in RTI-in compared to RTI-out is greater for neurons in which HFI predicted rate tuning compared to neurons in which duration tuning predicted rate tuning ($\eta^2 = 0.84$ *versus* $\eta^2 = 0.56$). Fig. 6B provides further support for this assessment. The difference in RTI (RTI-out–RTI-in) was compared between neurons in which HFI explained rate selectivity and neurons in which duration tuning explained rate selectivity. The reduction in RTI in duration tuned neurons was significantly smaller than in the neurons with HFI (Fig. 6B, two-sample t-test, $t = 2.56$, $p < 0.05$). The RTI-out *versus* RTI-in comparison shows that even in duration tuned neurons, putative HFI sidebands may contribute to rate selectivity.

To measure how well sideband inhibition and duration tuning predicted observed rate selectivity, a 'prediction accuracy' was calculated as follows:

$$\text{PA} = |(\text{observed 50\% cutoff} - \text{predicted 50\% cutoff})|/\text{observed 50\% cutoff}$$

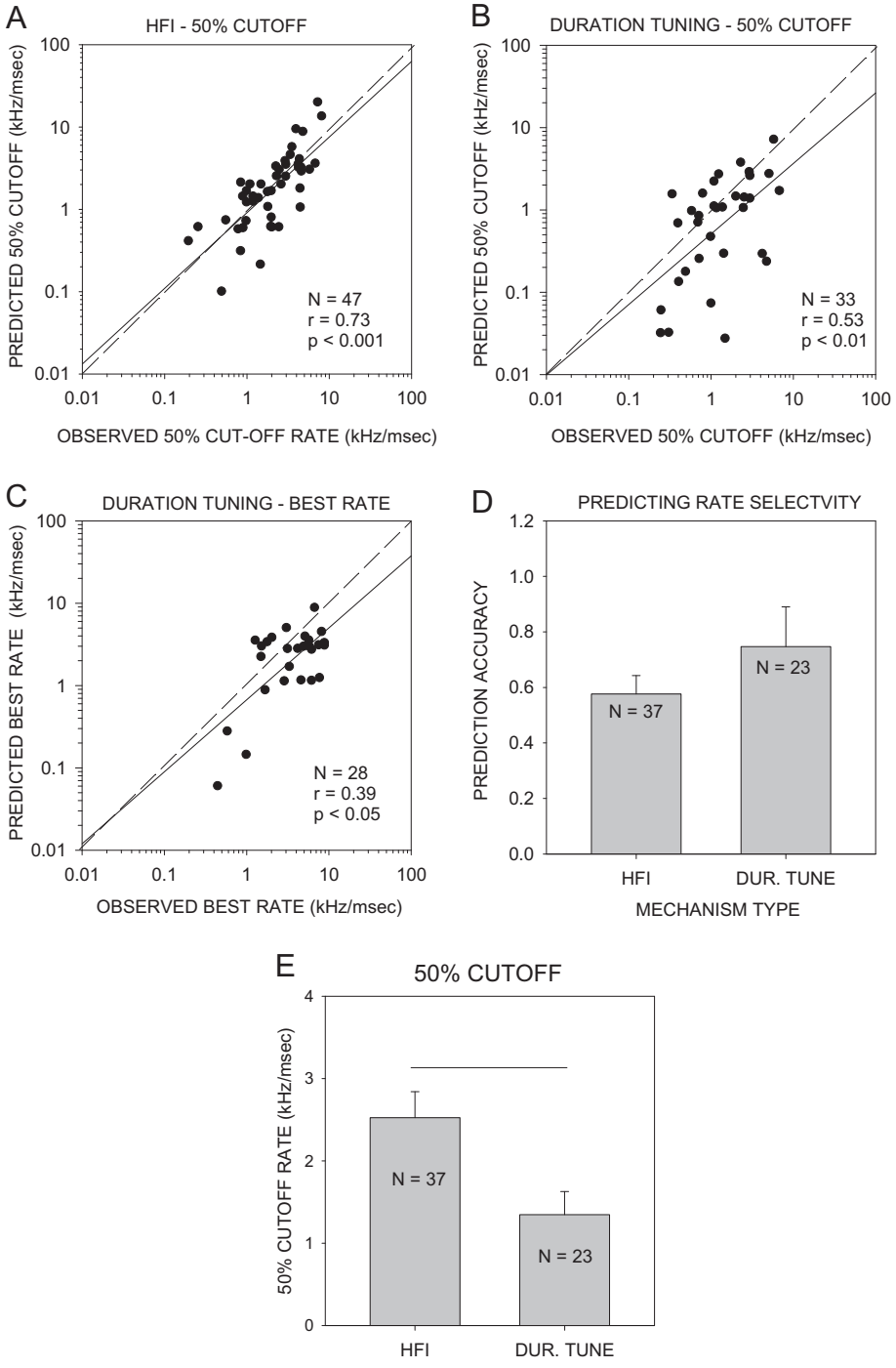

Fig. 5. Population data. (A) Properties of HFI bandwidth and arrival time predicted the 50% cutoff rate for FP and BP rate tuned neurons. A Pearson correlation revealed a significant correlation ($r = 0.73$, $p < 0.001$). The diagonal line represents the regression line. The diagonal dashed line represents the unity slope line. (B) An interaction between the 50% cutoff duration for short-pass-DT neurons and the excitatory tuning bandwidth predicted the 50% cutoff in FP and BP neurons. A Pearson correlation revealed a significant correlation ($r = 0.53$, $p < 0.01$). The diagonal dashed line represents unity slope. (C) An interaction between the best duration and tuning bandwidth predicted the best rate for BP neurons. A Pearson correlation revealed that the correlation was significant ($r = 0.39$, $p < 0.05$). The diagonal dashed line represents the unity slope line. (D) Mean (±SEM) prediction accuracy. The bar titled "HFI" represents neurons where HFI was present and the bar titled "DUR. TUNE" represents neurons where short-pass duration tuning was present. Prediction accuracy did not differ between HFI and duration tuned neurons ($t = -1.21$, $p = 0.23$) indicating that duration tuning and HFI predicted 50% cutoff equally well. (E) Mean (±SEM) 50% cutoff rate for FP and BP neurons. A two-sample t-test revealed that duration tuned neurons had a significantly slower 50% cutoff rate compared to HFI neurons ($t = 2.57$, $p < 0.05$).

The prediction accuracy did not depend on which mechanism shaped rate selectivity (Fig. 5D, $t = 1.21$, $p = 0.23$) indicating that when present either response property predicted rate selectivity similarly.

We conclude that sideband inhibition is the main response property shaping FM rate selectivity simply because HFI was present in a larger percentage of neurons (~88%) than duration tuning (34%). The distribution of these two mechanisms was not CF-dependent. A t-test between the CF of neurons in which duration tuning predicted rate selectivity and neurons that depended on HFI revealed no significant difference ($t = -1.2$, $p = 0.23$).

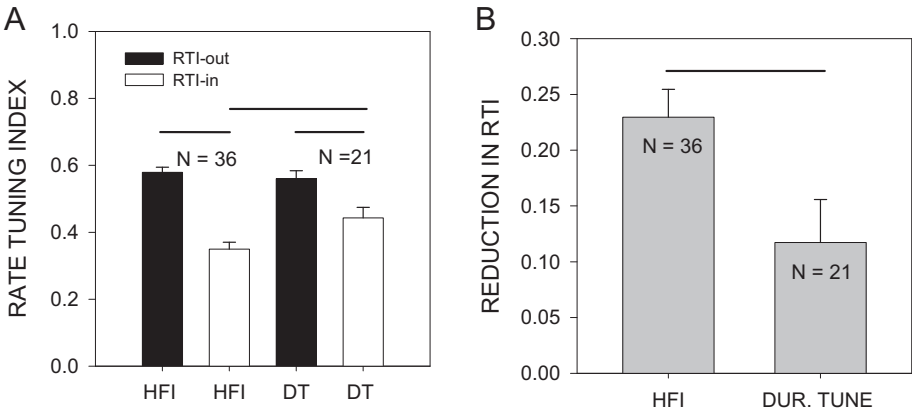

Fig. 6. RTI is influenced by sweep bandwidth to different degrees in neurons with HFI *versus* duration tuned neurons. (A) The RTI for sweeps that start outside the excitatory tuning curve (black bars: RTI-out) was compared with RTI for sweeps that start inside the tuning curve (white bars: RTI-in). The horizontal bars represent comparisons for which a *t*-test revealed significant difference ($p < 0.05$). In neurons in which HFI predicted rate selectivity, a paired *t*-test revealed that RTI-in was significantly lower than RTI-out ($t = 9.22$, $p < 0.001$, $\eta^2 = 0.84$). RTI-in was also lower than RTI-out for neurons in which duration tuning predicted rate selectivity ($t = 2.92$, $p < 0.01$, $\eta^2 = 0.56$), but the reduction in duration tuned neurons was significantly smaller than the reduction seen in neurons with HFI (comparison of effect sizes: $\eta^2 = 0.84$ *versus* $\eta^2 = 0.56$). (B) Mean (±SEM) reduction of RTI (RTI Out−RTI In) for the neurons represented in (A). A two-sample *t*-test revealed that RTI-in is reduced compared to RTI-out to a significantly greater extent in neurons with HFI relative to duration tuned neurons ($t = 2.56$, $p < 0.05$).

Therefore, these mechanisms are likely to be found anywhere along the tonotopic axis. However, neurons that depended on HFI and duration tuning for rate tuning exhibited significantly different 50% cutoff rates. The observed 50% cutoff rate was slower for duration tuned neurons than for HFI neurons (Fig. 5E, two-sample *t*-test, $t = 2.57$, $p < 0.05$). This indicates differences in response selectivity shaped by each mechanism.

3.3. A minority of neurons exhibited both HFI and duration tuning

Whether both sideband inhibition and duration tuning were present in the same neuron was assessed in 32 neurons that had HFI. Ten (~31%) of these neurons were also duration tuned. This level of duration tuning was consistent with the ~34% duration tuning found in the overall population of BP/FP sweep selective neurons. The presence of both properties in the same neurons raises the question of whether these mechanisms independently predict rate selectivity or if they add to each other in some manner. Fig. 7 shows a representative neuron with CF tone duration tuning (Fig. 7A, best duration ~3 msec). The neuron also exhibited HFI, with arrival time of 1.6 msec and a bandwidth of 5 kHz (Fig. 7B). The neuron was BP selective for FM sweep rates (Fig. 7C). The predicted 50% cutoff using duration tuning (2.6 kHz/ms) or using HFI (3.2 kHz/ms) were similar to the observed 50% cutoff rate (4.1 kHz/

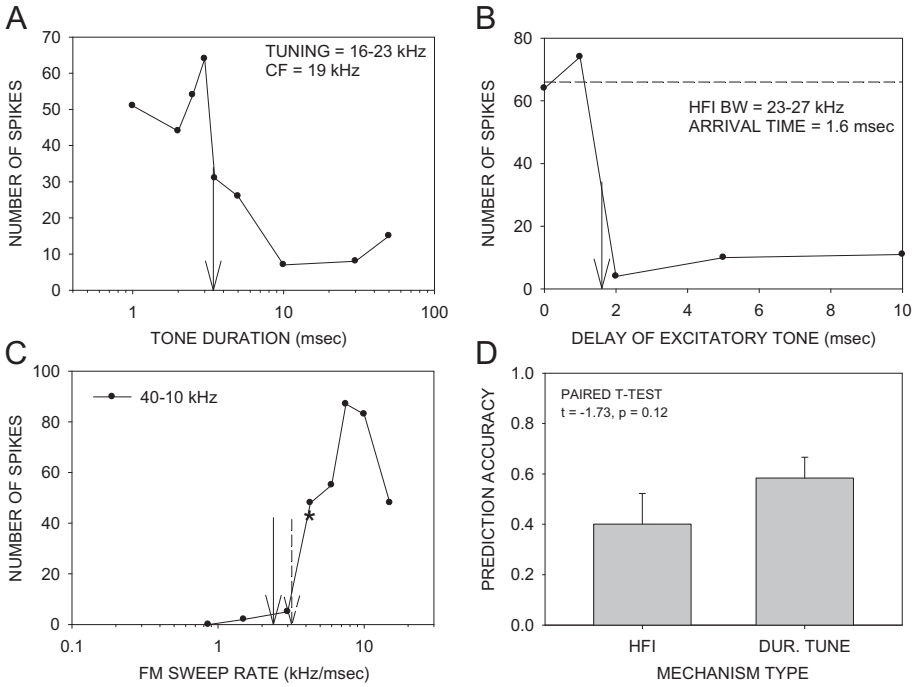

Fig. 7. Neurons in which both mechanisms were present. (A–C) An example neuron in which both duration tuning and HFI were present. (A) The neuron was duration tuned for CF tone (19 kHz). The 50% tone duration (vertical arrow) was 3.2 msec and the tuning curve bandwidth was 16–23 kHz, predicting a 50% cutoff of 2.5 kHz/ms (solid arrow in C). (B) The neuron also exhibited HFI with an arrival time of inhibition of 1.6 msec (vertical arrow). The bandwidth of inhibition was 5 kHz, predicting a 50% cutoff of 3.1 kHz/ms (dashed arrow in C). (C) The observed rate selectivity function of this neuron. The observed 50% cutoff was 4.1 kHz/ms (asterisk in C). (D) The prediction accuracy for the 10 neurons in which both mechanisms were present. The bar titled 'HFI' was obtained by using HFI to predict the 50% cutoff and the bar titled 'DUR. TUNE' was obtained by using duration tuning to predict. A paired *t*-test revealed no significant difference between the two predictions ($t = -1.73$, $p = 0.12$) indicating that both mechanisms independently predict rate tuning similarly.

ms). An analysis of prediction accuracy for the 10 neurons using each mechanism showed that HFI and duration tuning individually predict similar rate selectivity in these neurons (Fig. 7D, paired t-test, $t = -1.73$, $p = 0.12$).

4. Discussion

At least two different response properties predict downward FM sweep rate selectivity in the core auditory cortex of the young C57 mouse: sideband inhibition and duration tuning. Although both properties predicted rate selectivity equally well, sideband inhibition was found in more neurons tested (~88%) than duration tuning (34%). On average, neurons in which duration tuning predicted rate selectivity exhibited a slower 50% cutoff rate compared to neurons that depended on HFI (Fig. 5E). The 50% cutoff rate is approximately the center of the range of rates that produce maximal change in response magnitude in a neuron. Therefore, it is the rate around which the neuron provides maximal information (Harper and McAlpine, 2004). This suggests that sideband inhibition and duration tuning result in maximum information about FM sweep rates over different, but overlapping, ranges of rates. In addition, the sweep bandwidth influenced rate tuning to a greater degree in neurons that depended on HFI compared to neurons that depended on duration tuning for rate tuning (Fig. 6). Thus the two mechanisms produced different rate selectivity properties.

4.1. Duration tuning for tones in the auditory system

The relative scarcity of band- and short-pass duration tuning in the mouse A1 is consistent with similar findings in the mouse and chinchilla IC (Brand et al., 2000; Chen, 1998), the pallid bat A1 (Razak and Fuzessery, 2006) and the cat cortical dorsal zone (He et al., 1997). This differs from findings in little brown bat A1 (Galazyuk and Feng, 1997), pallid bat and big brown bat IC (Casseday et al., 1994; Fuzessery et al., 2006) in which ~30–60% of neurons exhibit short- and band-pass duration tuning. Thus, comparative data in general point to more duration tuning in the midbrain of bats compared to auditory cortex across species, although the little brown bat data serve as an exception to this generalization.

Duration tuning has been typically proposed as a temporal feature detector for conspecific vocalizations (Brand et al., 2000; Feng et al., 1990; Gooler and Feng, 1992). In frogs for example, neurons in the auditory midbrain have been postulated to code for durations of mating calls or the amplitude modulations contained within them (Feng et al., 1990; Gooler and Feng, 1992). Fuzessery et al. (2006) suggested an additional role for duration tuning. Duration tuning for tones in the pallid bat IC predicts FM rate selectivity. According to this model, sweeps with rates that stimulate the excitatory tuning curve at the optimal duration will elicit maximum response. For slower and faster sweeps, the excitatory tuning curve will be stimulated over non-optimal durations, and thus such rates elicit reduced responses. This was found to be the case in the mouse auditory cortex as well in which CF duration tuning and width of excitatory tuning curve predicted FM rate selectivity in ~33% of neurons. Thus, duration tuning in the auditory system may serve to establish both temporal and spectrotemporal filters across taxa.

4.2. Sideband inhibition in the auditory system

Sideband inhibition is common in the auditory cortex across species (Brosch and Schreiner, 1997; Calford and Semple, 1995; Razak and Fuzessery, 2006; Suga, 1965; Sutter and Loftus, 2003; Wu et al., 2008; Zhang et al., 2003). The role of sideband inhibition in FM sweep rate selectivity was investigated in detail in the auditory system of bats (Gordon and O'Neill, 1998; Fuzessery et al., 2006; Razak and Fuzessery, 2006). In these studies, it was shown that the spectrotemporal interactions between excitatory tuning curve and inhibitory sidebands shaped FM sweep direction and rate selectivity. In the pallid bat A1, this was the dominant mechanism of sweep direction and rate selectivity. The present data on mouse cortex indicates that similar properties shape selectivity across auditory generalists and specialists. This study was limited to mechanisms shaping rate selectivity for downward sweeps and therefore focused on the HFI sideband. Most neurons in the mouse auditory cortex respond similarly to up and down sweeps (Trujillo et al., 2011). Therefore, it is predicted that the properties of sideband on the low-frequency side are similar to those on the high-frequency side. In direction selective cells, asymmetries in properties of sidebands may be present (Razak and Fuzessery, 2006). Wu et al. (2008) suggested that sideband inhibition is shaped by rapid spiking interneurons commonly identified as Parvalbumin positive. These neurons are known to be involved in shaping selectivity for rapid temporal features of sound (Atencio and Schreiner, 2008), consistent with the notion proposed here that sideband inhibition shapes selectivity for fast or medium sweep rates.

It is unclear if the observed sideband inhibition and duration tuning are computed at the level of the cortex or whether these properties are inherited from subcortical computations. In aging rats, FM sweep rate selectivity is reduced in the auditory cortex but not in the midbrain or thalamus (Lee et al., 2002; Mendelson and Lui, 2004; Mendelson and Ricketts, 2001). This suggests that at least some of the mechanisms shaping sweep rate selectivity in rodent A1 are local. Iontophoretic application of GABAa receptor antagonists has shown that sideband inhibition is shaped at the level of the IC (Fuzessery and Hall, 1996) as well as in A1 (Razak and Fuzessery, 2009). The iontophoresis data also indicate that synaptic inhibition is an important mechanism for sideband inhibition, although other factors such as mechanical suppression in cochlea (Ruggero et al., 1992) and synaptic depression (Wehr and Zador, 2005) may contribute.

Sideband inhibition with the potential to influence FM responses is also present in the cochlear nucleus (Shofner and Young, 1985) and selective responses to FM type stimuli have been observed in the cochlear nucleus (Moller, 1974). This indicates that FM sweep rate and direction selectivity may be shaped and refined at multiple levels of the auditory system. Therefore, even though a response property is present at a lower level in the pathway, the higher processing level may not simply inherit the property. This may be necessary due to convergence of pathways that smear selectivity (McMullen and de Venecia, 1993; Middlebrooks and Zook, 1983) necessitating refinement using local inhibitory circuits. At least for thalamocortical pathways, this is consistent with data from Miller et al. (2001) who showed that excitatory properties are more faithfully transmitted from thalamus to A1 compared to inhibitory properties.

4.3. Comparison to previous studies of auditory and other sensory systems

In the bat auditory system, sideband inhibition, facilitation and duration tuning shape FM rate selectivity (Gordon and O'Neill, 1998; Razak and Fuzessery, 2006). Other mechanisms such as relative amplitudes of inhibitory/excitatory conductance of inputs and spike threshold also contribute (Gittelman and Pollak, 2011). Properties of sideband inhibition have also been suggested to shape FM sweep rate and direction selectivity in the monkey, cat, ferret

and rat A1 (Atencio et al., 2007; Nelken and Versnel, 2000; Phillips et al., 1985; Sadagopan and Wang, 2010; Zhang et al., 2003). The mouse auditory cortex is similar to the pallid bat A1 in that sideband inhibition is the dominant mechanism. However, these two systems differ in that duration tuning, largely absent in the pallid bat cortex, is present and predicts rate selectivity in the mouse auditory cortex.

Selectivity for FM sweep rate is analogous to movement velocity selectivity in the visual system. Two of the mechanisms proposed to underlie velocity selectivity are fundamentally similar to those in the mouse and the bat auditory systems. These are spatiotemporal asymmetries in lateral inhibition (superior colliculus – (Razak and Pallas, 2005); visual cortex – (Duysens et al., 1985a, 1985b; Patel and Sillito, 1978)) and tuning for the duration that a stimulus spends in the receptive field (Duysens et al., 1996). These similarities across auditory and visual systems indicate that multiple, but similar, solutions are used to solve analogous problems.

4.4. Methodological considerations

These data have to be interpreted within the context of at least three methodological issues. The first is that mechanisms were assessed under ketamine/xylazine/isoflurane anesthesia. In the auditory cortex, ketamine reduces spontaneous and sound-evoked activity (Syka et al., 2005; Zurita et al., 1994). Thus it is likely that response magnitudes reported in this study are under-estimates relative to responses from awake animals. The second issue is the use of linear FM sweeps as stimuli. Nelken and Versnel (2000) compared ferret A1 responses to linear and logarithmic sweeps and found that FM rate selectivity did not differ based on the type of sweep, suggesting the sweep trajectory may not have a bearing on the results reported here. The third issue is that the focus was only on mechanisms underlying FP and BP selectivity for downward sweeps. It is likely that additional mechanisms exist to shape slow-pass FM rate selectivity.

5. Conclusions

These data show that neural selectivity for FM sweeps can be predicted based on linear interactions between two tones (sideband inhibition) or temporal selectivity for individual excitatory tones (duration tuning). Because the C57 strain is a mouse model of presbycusis, these data provide the baseline for investigations of how basic spectrotemporal processing changes due to presbycusis. While both duration tuning and sideband inhibition depend on interactions between excitation and inhibition, they differ in one fundamental way. According to the scheme of (Happel et al., 2010) duration tuning can be thought of as arising due to on-CF and near-CF interactions between excitation and inhibition. Sidebands, by definition, arise from non-CF and on-CF interactions. Some of these non-CF inputs are inhibitory and may generate the inhibitory sidebands (Kaur et al., 2005). Given the link between fast temporal processing, sideband inhibition and Parvalbumin-expressing interneurons (Wu et al., 2008; Atencio and Schreiner, 2008), and the observed reduction of Parvalbumin-expressing cells in presbycusis (Martin del Campo et al., 2012; Ouda et al., 2008), reduction in selectivity for fast temporal modulations in presbycusis (Lee et al., 2002; Mendelson and Lui, 2004; Mendelson and Ricketts, 2001) may be related to loss of sidebands. In presbycusis, the loss of response to high-frequencies suggests that the HFI-based mechanism will be more susceptible to aging and hearing loss compared to duration tuning. The extent to which these two mechanisms are differentially plastic in presbycusis and the relevance to FM sweep processing is currently being investigated.

Acknowledgments

We thank the members of the Razak lab for useful discussions of the data and Dr. Peter Hickmott for feedback on an earlier version of the paper. Funding for this study was provided by the Deafness Research Foundation and University of California, Riverside.

References

Atencio, C.A., Blake, D.T., Strata, F., Cheung, S.W., Merzenich, M.M., Schreiner, C.E., 2007. Frequency-modulation encoding in the primary auditory cortex of the awake owl monkey. J. Neurophysiol. 98, 2182–2195.
Atencio, C.A., Schreiner, C.E., 2008. Spectrotemporal processing differences between auditory cortical fast-spiking and regular-spiking neurons. J. Neurosci. 28, 3897–3910.
Barkat, T., Polley, D., Hensch, T., 2011. A critical period for auditory thalamocortical connectivity. Nat. Neurosci. 14, 1189–1194.
Brand, A., Urban, R., Grothe, B., 2000. Duration tuning in the mouse auditory midbrain. J. Neurophysiol. 84, 1790–1799.
Brosch, M., Schreiner, C.E., 1997. Time course of forward masking tuning curves in cat primary auditory cortex. J. Neurophysiol. 77, 923–943.
Brown, T., Harrison, R.V., 2009. Responses of neurons in chinchilla auditory cortex to frequency-modulated tones. J. Neurophysiol. 101, 2017–2029.
Calford, M.B., Semple, M.N., 1995. Monaural inhibition in cat auditory cortex. J. Neurophysiol. 73, 1876–1891.
Caspary, D.M., Ling, L., Turner, J.G., Hughes, L.F., 2008. Inhibitory neurotransmission, plasticity and aging in the mammalian central auditory system. J. Exp. Biol. 211, 1781–1791.
Casseday, J.H., Ehrlich, D., Covey, E., 2000. Neural measurement of sound duration: control by excitatory-Inhibitory interactions in the inferior colliculus. J. Neurophysiol. 84, 1475–1487.
Casseday, J.H., Ehrlich, D., Covey, E., 1994. Neural tuning for sound duration: role of inhibitory mechanisms in the inferior colliculus. Science 264, 847–850.
Chen, G.-D., 1998. Effects of stimulus duration on responses of neurons in the chinchilla inferior colliculus. Hear. Res. 122, 142–150.
Cruikshank, S.J., Killackey, H.P., Metherate, R., 2001. Parvalbumin and calbindin are differentially distributed within primary and secondary subregions of the mouse auditory forebrain. Neuroscience 105, 553–569.
Duysens, J., Orban, G.A., Cremieux, J., Maes, H., 1985a. Velocity selectivity in the cat visual system. III. Contribution of temporal factors. J. Neurophysiol. 54, 1068–1083.
Duysens, J., Orban, G.A., Cremieux, J., Maes, H., 1985b. Visual cortical correlates of visible persistence. Vision Res. 25, 171–178.
Duysens, J., Schaafsma, S.J., Orban, G.A., 1996. Cortical off response tuning for stimulus duration. Vision Res. 36, 3243–3251.
Ehrlich, D., Casseday, J.H., Covey, E., 1997. Neural tuning to sound duration in the inferior colliculus of the big brown bat, Eptesicus fuscus. J. Neurophysiol. 77, 2360–2372.
Erway, L.C., Willott, J.F., Archer, J.R., Harrison, D.E., 1993. Genetics of age-related hearing loss in mice: I. Inbred and F1 hybrid strains. Hear. Res. 65, 125–132.
Felsheim, C., Ostwald, J., 1996. Responses to exponential frequency modulations in the rat inferior colliculus. Hear. Res. 98, 137–151.
Feng, A.S., Hall, J.C., Gooler, D.M., 1990. Neural basis of sound pattern recognition in anurans. Prog. Neurobiol. 34, 313–329.
Frisina, D.R., Frisina, R.D., 1997. Speech recognition in noise and presbycusis: relations to possible neural mechanisms. Hear. Res. 106, 95–104.
Fuzessery, Z.M., Hall, J.C., 1996. Role of GABA in shaping frequency tuning and creating FM sweep selectivity in the inferior colliculus. J. Neurophysiol. 76, 1059–1073.
Fuzessery, Z.M., Hall, J.C., 1999. Sound duration selectivity in the pallid bat inferior colliculus. Hear. Res. 137, 137–154.
Fuzessery, Z.M., Richardson, M.D., Coburn, M.S., 2006. Neural mechanisms underlying selectivity for the rate and direction of frequency-modulated sweeps in the inferior colliculus of the pallid bat. J. Neurophysiol. 96, 1320–1336.
Galazyuk, A.V., Feng, A.S., 1997. Encoding of sound duration by neurons in the auditory cortex of the little brown bat, Myotis lucifugus. J. Comp. Physiol. A Neuroethol. Sens. Neural. Behav. Physiol. 180, 301–311.
Galindo-Leon, E.E., Lin, F.G., Liu, R.C., 2009. Inhibitory plasticity in a lateral band improves cortical detection of natural vocalizations. Neuron, 705–716.
Gittelman, J.X., Li, N., 2011. FM velocity selectivity in the inferior colliculus is inherited from velocity-selective inputs and enhanced by spike threshold. J. Neurophysiol. 106, 2399–2414.
Gittelman, J.X., Pollak, G.D., 2011. It's about time: how input timing is used and not used to create emergent properties in the auditory system. J. Neurosci. 31, 2576–2583.
Godey, B., Atencio, C.A., Bonham, B.H., Schreiner, C.E., Cheung, S.W., 2005. Functional organization of squirrel monkey primary auditory cortex: responses to frequency-modulation sweeps. J. Neurophysiol. 94, 1299–1311.
Gooler, D.M., Feng, A.S., 1992. Temporal coding in the frog auditory midbrain: the influence of duration and rise-fall time on the processing of complex amplitude-modulated stimuli. J. Neurophysiol. 67, 1–22.

Gordon, M., O'Neill, W.E., 1998. Temporal processing across frequency channels by FM selective auditory neurons can account for FM rate selectivity. Hear. Res. 122, 97–108.
Hall, D.A., Haggard, M.P., Akeroyd, M.A., Summerfield, A.Q., Palmer, A.R., Elliott, M.R., Bowtell, R.W., 2000. Modulation and task effects in auditory processing measured using fMRI. Hum. Brain Map 10, 107–119.
Happel, M.F.K., Jeschke, M., Ohl, F.W., 2010. Spectral integration in primary auditory cortex attributable to temporally precise convergence of thalamocortical and intracortical input. J. Neurosci. 30, 11114–11127.
Harper, N.S., McAlpine, D., 2004. Optimal neural population coding of an auditory spatial cue. Nature 430, 682–686.
He, J., Hashikawa, T., Ojima, H., Kinouchi, Y., 1997. Temporal integration and duration tuning in the dorsal zone of cat auditory cortex. J. Neurosci. 17, 2615–2625.
Heil, P., Rajan, R., Irvine, D.R.F., 1992. Sensitivity of neurons in cat primary auditory cortex to tones and frequency-modulated stimuli. II: organization of response properties along the isofrequency dimension. Hear. Res. 63, 135–156.
Henry, K.R., Chole, R.A., 1980. Genotypic differences in behavioral, physiological and anatomical expressions of age-related hearing loss in the laboratory mouse. Audiology 19, 369–383.
Holmstrom, L.A., Eeuwes, L.B.M., Roberts, P.D., Portfors, C.V., 2010. Efficient encoding of vocalizations in the auditory midbrain. J. Neurosci. 30, 802–819.
Hunter, K.P., Willott, J.F., 1987. Aging and the auditory brainstem response in mice with severe or minimal presbycusis. Hear. Res. 30, 207–218.
Johnson, K.R., Erway, L.C., Cook, S.A., Willott, J.F., Zheng, Q.Y., 1997. A major gene affecting age-related hearing loss in C57BL/6J mice. Hear. Res. 114, 83–92.
Johnson, K.R., Zheng, Q.Y., Erway, L.C., 2000. A major gene affecting age-related hearing loss is common to at least ten inbred strains of mice. Genomics 70, 171–180.
Kaur, S., Rose, H.J., Lazar, R., Liang, K., Metherate, R., 2005. Spectral integration in primary auditory cortex: laminar processing of afferent input, in vivo and in vitro. Neuroscience 134, 1033–1045.
Lee, H.J., Wallani, T., Mendelson, J.R., 2002. Temporal processing speed in the inferior colliculus of young and aged rats. Hear. Res. 174, 64–74.
Linden, J.F., Liu, R.C., Sahani, M., Schreiner, C.E., Merzenich, M.M., 2003. Spectrotemporal structure of receptive fields in areas AI and AAF of mouse auditory cortex. J. Neurophysiol. 90, 2660–2675.
Linden, J.F., Schreiner, C.E., 2003. Columnar transformations in auditory cortex? A comparison to visual and somatosensory cortices. Cereb. Cortex 13, 83–89.
Liu, R.C., 2006. Prospective contributions of transgenic mouse models to central auditory research. Brain Res. 1091, 217–223.
Martin del Campo, H., Measor, K., Razak, K.A., 2012. Parvalbumin immunoreactivity in the auditory cortex of a mouse model of presbycusis. Hear. Res. 294, 31–39.
Mataga, N., Fujishima, S., Condie, B.G., Hensch, T.K., 2001. Experience-dependent plasticity of mouse visual cortex in the absence of the neuronal activity-dependent marker egr1/zif268. J. Neurosci. 21, 9724–9732.
McMullen, N.T., de Venecia, R.K., 1993. Thalamocortical patches in auditory neocortex. Brain Res. 620, 317–322.
Mendelson, J.R., Cynader, M.S., 1985. Sensitivity of cat primary auditory cortex (AI) neurons to the direction and rate of frequency modulation. Brain Res. 327, 331–335.
Mendelson, J.R., Lui, B., 2004. The effects of aging in the medial geniculate nucleus: a comparison with the inferior colliculus and auditory cortex. Hear. Res. 191, 21–33.
Mendelson, J.R., Ricketts, C., 2001. Age-related temporal processing speed deterioration in auditory cortex. Hear. Res. 158, 84–94.
Mendelson, J.R., Schreiner, C.E., Sutter, M.L., Grasse, K.L., 1993. Functional topography of cat primary auditory cortex: responses to frequency-modulated sweeps. Exp. Brain Res. 94, 65–87.
Middlebrooks, J.C., Zook, J.M., 1983. Intrinsic organization of the cat's medial geniculate body identified by projections to binaural response-specific bands in the primary auditory cortex. J. Neurosci. 3, 203–224.
Mikaelian, D.O., 1979. Development and degeneration of hearing in the C57/b16 mouse: relation of electrophysiologic responses from the round window and cochlear nucleus to cochlear anatomy and behavioral responses. Laryngoscope 89, 1–15.
Miller, L.M., Escabí, M.A., Read, H.L., Schreiner, C.E., 2001. Functional convergence of response properties in the auditory thalamocortical system. Neuron 32, 151–160.
Moller, A.R., 1974. Coding of sounds with rapidly varying spectrum in the cochlear nucleus. J. Acoust. Soc. Am. 55, 631–640.
Morishita, H., Miwa, J.M., Heintz, N., Hensch, T.K., 2010. Lynx1, a cholinergic brake, limits plasticity in adult visual cortex. Science 1238, 1–4.
Nelken, I., Versnel, H., 2000. Responses to linear and logarithmic frequency-modulated sweeps in ferret primary auditory cortex. Eur. J. Neurosci. 12, 549–562.
Noben-Trauth, K., Zheng, Q.Y., Johnson, K.R., 2003. Association of cadherin 23 with polygenic inheritance and genetic modification of sensorineural hearing loss. Nat. Genet. 35, 21–23.
O'Connor, D.H., Huber, D., Svoboda, K., 2009. Reverse engineering the mouse brain. Nature 461, 923–929.
Ohl, F.W., Wetzel, W., Wagner, T., Rech, A., Scheich, H., 1999. Bilateral ablation of auditory cortex in Mongolian gerbil affects discrimination of frequency modulated tones but not of pure tones. Learn. Memory 6, 347–362.
Ouda, L., Druga, R., Syka, J., 2008. Changes in parvalbumin immunoreactivity with aging in the central auditory system of the rat. Exp. Gerontol. 43, 782–789.
Patel, H.H., Sillito, A.M., 1978. Inhibition and velocity tuning in the cat visual cortex. J. Physiol. 284, 113P–114P.
Phillips, D.P., Mendelson, J.R., Cynader, M.S., Douglas, R.M., 1985. Responses of single neurones in cat auditory cortex to time-varying stimuli: frequency-modulated tones of narrow excursion. Exp. Brain Res. 58, 443–454.
Poon, P.W.F., Chen, X., Hwang, J.C., 1991. Basic determinants for FM responses in the inferior colliculus of rats. Exp. Brain Res. 83, 598–606.
Razak, K.A., Fuzessery, Z.M., 2008. Facilitatory mechanisms underlying selectivity for the direction and rate of frequency modulated sweeps in the auditory cortex. J. Neurosci. 28, 9806–9816.
Razak, K.A., Fuzessery, Z.M., 2009. GABA shapes selectivity for the rate and direction of frequency-modulated sweeps in the auditory cortex. J. Neurophysiol. 102, 1366–1378.
Razak, K.A., Fuzessery, Z.M., 2006. Neural mechanisms underlying selectivity for the rate and direction of frequency-modulated sweeps in the auditory cortex of the pallid bat. J. Neurophysiol. 96, 1303–1319.
Razak, K.A., Pallas, S.L., 2005. Neural mechanisms of stimulus velocity tuning in the superior colliculus. J. Neurophysiol. 94, 3573–3589.
Ricketts, C., Mendelson, J.R., Anand, B., English, R., 1998. Responses to time-varying stimuli in rat auditory cortex. Hear. Res. 123, 27–30.
Ruggero, M.A., Robles, L., Rich, N.C., 1992. Two-tone suppression in the basilar membrane of the cochlea: mechanical basis of auditory-nerve rate suppression. J. Neurophysiol. 68, 1087–1099.
Sadagopan, S., Wang, X., 2010. Contribution of inhibition to stimulus selectivity in primary auditory cortex of awake primates. J. Neurosci. 30, 7314–7325.
Shamma, S.A., Fleshman, J.W., Wiser, P.R., Versnel, H., 1993. Organization of response areas in ferret primary auditory cortex. J. Neurophysiol. 69, 367–383.
Shofner, W.P., Young, E.D., 1985. Excitatory/inhibitory response types in the cochlear nucleus: relationships to discharge patterns and responses to electrical stimulation of the auditory nerve. J. Neurophysiol. 54, 917–939.
Spongr, V.P., Flood, D.G., Frisina, R.D., Salvi, R.J., 1997. Quantitative measures of hair cell loss in CBA and C57BL/6 mice throughout their life spans. J. Acoust. Soc. Am. 101, 3546–3553.
Stiebler, I., Neulist, R., Fichtel, I., Ehret, G., 1997. The auditory cortex of the house mouse: left-right differences, tonotopic organization and quantitative analysis of frequency representation. J. Comp. Physiol. A Neuroethol. Sens. Neural. Behav. Physiol. 181, 559–571.
Suga, N., 1965. Responses of cortical auditory neurones to frequency modulated sounds in echo-locating bats. Nature 206, 890–891.
Sugiyama, S., Nardo Aa, Di, Aizawa, S., Matsuo, I., Volovitch, M., Prochiantz, A., Hensch, T.K., 2008. Experience-dependent transfer of Otx2 homeoprotein into the visual cortex activates postnatal plasticity. Cell 134, 508–520.
Sutter, M.L., Loftus, W.C., 2003. Excitatory and inhibitory intensity tuning in auditory cortex: evidence for multiple inhibitory mechanisms. J. Neurophysiol. 90, 2629–2647.
Syka, J., Suta, D., Popelar, J., 2005. Responses to species-specific vocalizations in the auditory cortex of awake and anesthetized guinea pigs. Hear. Res. 206, 177–184.
Taberner, A.M., Liberman, M.C., 2005. Response properties of single auditory nerve fibers in the mouse. J. Neurophysiol. 93, 557–569.
Tian, B., Rauschecker, J.P., 1994. Processing of frequency-modulated auditory field sounds in the cat's anterior. Surgery 71.
Tian, B., Rauschecker, J.P., 2004. Processing of frequency-modulated sounds in the lateral auditory belt cortex of the rhesus monkey. J. Neurophysiol. 92, 2993–3013.
Trujillo, M., Measor, K., Carrasco, M.M., Razak, K.A., 2011. Selectivity for the rate of frequency-modulated sweeps in the mouse auditory cortex. J. Neurophysiol. 106, 2825–2837.
Washington, S.D., Kanwal, J.S., 2008. DSCF neurons within the primary auditory cortex of the mustached bat process frequency modulations present within social calls. J. Neurophysiol. 100, 3285–3304.
Wehr, M., Zador, A.M., 2005. Synaptic mechanisms of forward suppression in rat auditory cortex. Neuron 47, 437–445.
Wetzel, W., Wagner, T., Ohl, F.W., Scheich, H., 1998. Categorical discrimination of direction in frequency-modulated tones by Mongolian gerbils. Behav. Brain Res. 91, 29–39.
Whitfield, I.C., Evans, E.F., 1965. Responses of auditory cortical neurons to stimuli of changing frequency. J. Neurophysiol. 28, 655–672.
Willott, J.F., 1986. Effects of aging, hearing loss, and anatomical location on thresholds of inferior colliculus neurons in C57BL/6 and CBA mice. J. Neurophysiol. 56, 391–408.
Willott, J.F., Aitkin, L.M., McFadden, S.L., 1993. Plasticity of auditory cortex associated with sensorineural hearing loss in adult C57BL/6J mice. J. Comp. Neurol. 329, 402–411.
Wu, G.K., Arbuckle, R., Liu, B.-H., Tao, H.W., Zhang, L.I., 2008. Lateral sharpening of cortical frequency tuning by approximately balanced inhibition. Neuron 58, 132–143.
Zhang, L.I., Tan, A.Y.Y., Schreiner, C.E., Merzenich, M.M., 2003. Topography and synaptic shaping of direction selectivity in primary auditory cortex. Nature 424, 201–205.
Zurita, P., Villa, A.E.P., de Ribaupierre, Y., de Ribaupierre, F., Rouiller, E.M., 1994. Changes of single unit activity in the cat's auditory thalamus and cortex associated to different anesthetic conditions. Neurosci. Res. 19, 303–316.